OTOLITH IMAGE ANALYSIS BY COMPUTER VISION

Anatole Chessel, Ronan Fablet
IFREMER/LASAA, France

Charles Kervrann, Frederic Cao
IRISA/VISTA, France

Keywords: Computer vision, otolith, fish biology and ecology, biological image analysis, detection a contrario, variational methods.

Abstract: Otoliths are small stone located in fish inner ears and characterised by an accretionnary growth. They act as a biological archive and are of much use in marine biology and ecology. In this article a computer vision framework is presented which recover the successive shapes of the otolith and the significant ridges and valleys from a 2D grayscale image. Seeing vision processes as complex systems, an iterated process is presented using two perceptual information, contrast and good continuity. The successive concentric shapes of the otoliths are recovered as the level-sets of a dome shaped potential function, computed in a variational framework. Potential applications includes in particular fish age estimation, otoliths morphogenesis modelling, otolith proxy fusion.

1 INTRODUCTION

Otolith are small stones located in fish inner ears used for their spatial localisation. They grow continuously according to an accretionnary process. As the accretionary deposit is influenced both by physiological parameters and environmental conditions, fish otoliths can be viewed as biological archives from which a lot can be learned on fish biology and ecology. For instance, individual age data, which are among the key data for fish stock assessment, are estimated from the interpretation of fish otoliths.

The decoding of this biological archive is a difficult task, as the conditions influencing the accretion are numerous, and their effects not well known (Panfili et al., 2002). Various means of analysis of the physical and chemical properties of the stone can be used: microchemical analysis, mass or raman spectroscopy etc... Visual analysis of images of magnified otolith sections are also used but, being done by human operator, they would benefit a lot from computer vision techniques to improve automatising, robustness and quantitative evaluation. Such techniques would allow to fully consider the image as yet another mean of quantitative measurements similar for instance to chemical signatures (Panfili et al., 2002).

An otolith image can be seen in Figure 1. Concentric structures akin to the one found in tree trunk section can clearly be seen. Several works have tried to extract those curves, using multi-agent methods (Guillau et al., 2002) or active contours (Troadec et al., 2000). While yielding good results on the species considered as easy by expert (like plaice), they failed on more complicated images (like pollock or hake), because the hypothesis made were too restrictive.

The vision of concentric structures in otolith images are the result of complex global interactions between heterogeneous visual cues interpreted by the human vision system : what we see are continuous and smooth parallel concentric curves forming quasi-convex shapes. The analysis of low-level vision processes will lead to the definition of an original approach for the extraction of the relevant curves, and the recovery of the successive shapes of the otolith during its growth. Thus a novel framework for geometric images understanding applied to otoliths is proposed, the results of which can be seen in Fig. 1.

This paper is organized as follow. The next section presents a psychovisual analysis of otoliths and an overview of the framework with which we implement its conclusion. In section 3 the different steps are detailed. The last section details the implementation and shows results on several species.

Chessel A., Fablet R., Kervrann C. and Cao F. (2008).
OTOLITH IMAGE ANALYSIS BY COMPUTER VISION.
In *Proceedings of the First International Conference on Bio-inspired Systems and Signal Processing*, pages 490-497
DOI: 10.5220/0001067204900497

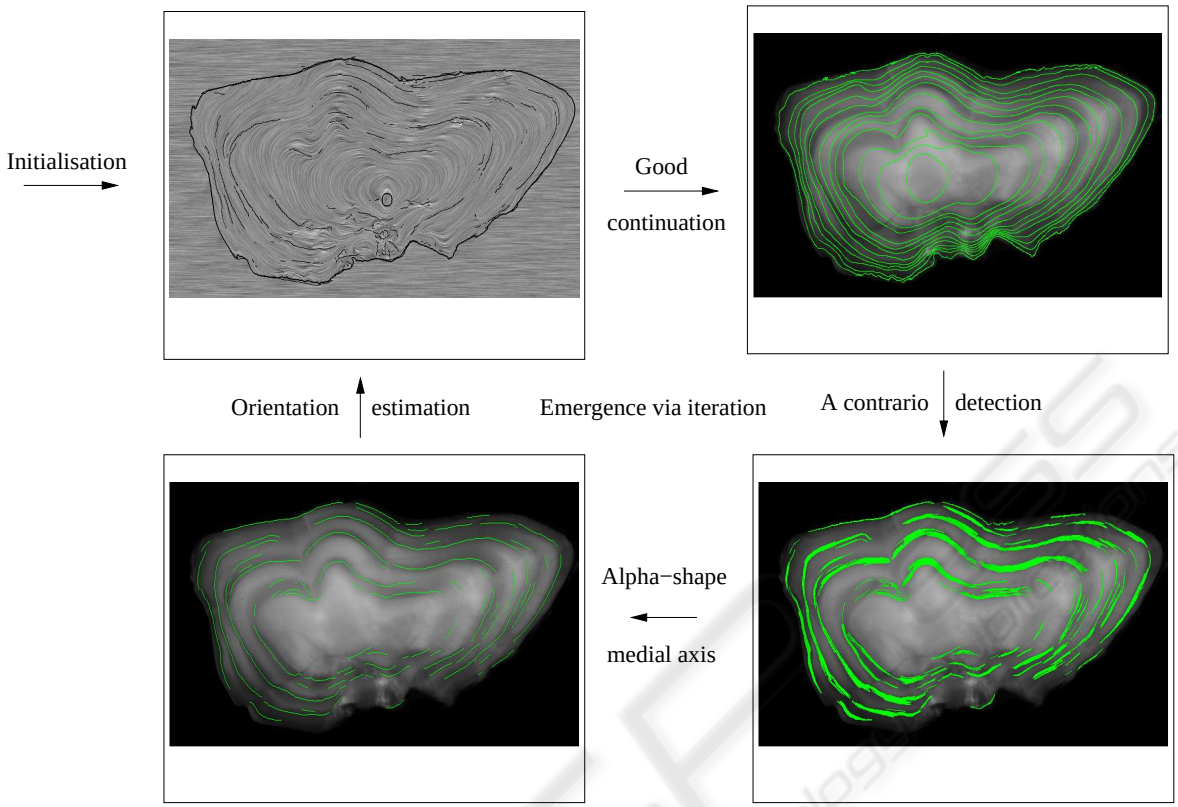

Figure 1: Overview of the process.

2 PSYCHOVISION AND CURVE EXTRACTION IN OTOLITHS

Psychovision is the study of vision from a subjective point of view: how do we manage to organize the wealth of information that reaches the retina into coherent structures? It is based on experiments where subjects are asked to describe how they perceive given stimuli. This section will be devoted to what psychovision can teach us about otolith images and how we can apply it in practice.

2.1 Perceptual Emergence from Interaction

Low-level vision is the part of vision (either biological or computer) that builds global structures (or percepts) i.e. curves, regions, depth perception, etc... from atomistic information, the pixels in one case and the cones and rods of the retina in the other. This process has been much studied, in particular by the Gestalt school of visual perception (Kanizsa, 1979).

They described the transition from local information to global percepts as the action of a number of grouping laws stating that individual cues having similar or compatible characteristics are seen as being part of the same group (Kanizsa, 1979). Those characteristics include color, direction, spatial proximity, global shape priors or specific structuring patterns like T-junction and X-junction.

But those laws interact one with the others, either reinforcing one another if they correspond to the same object, or inhibiting or masking one another if several interpretations of a scene are possible. Thus low-level vision can be seen as the process in which global percepts *emerge* from the complex interactions between perceptual cues and group of perceptual cues.

This description is based on the notion of emergence, which is characterised by the existence, in a hierarchy of organizational levels, of properties at a given level which are not explainable by/ reducible to the individual properties of elements of the lower levels. It is characteristic of *complex systems* (Benkirane, 2002). Such systems are notoriously difficult to understand and model because, every element being tied in non-linear ways with a great number of others, it is hard and/or unhelpful to try and study them separately.

2.2 Psychovisual Analysis of Otoliths

Otoliths are in some sense closer to artificial images used in psychovisual experiments than to natural ones. They are strongly organized geometrically in concentric curves alternatively darker and lighter which, despite a low contrast and various noises, are clearly seen event by an untrained eye. A number of grouping laws are involved in that perception: good continuation, concentricity and parallelism of the curves, quasi-convexity of the shapes, constant width of the rings. As all those informations describe the same structures, they reinforce one another, in positive feedback loops.

But most of those grouping laws work on a global scale. The problem might seem easy because otolith images are easily described subjectively as concentric curves, but saying so would be being triked by the ability of human vision to disregard all the cues that do not match its global view of an object. A careful analysis (or indeed any computer program which would lack that particular ability of the human eye) shows that there is locally a number of details that go against that interpretation, like flat zones, bubbles or isolated orthoradial structures. In the case of otoliths, two cues are mainly used: orientation, via the good continuation gestalt, and maxima of contrast. The proposed framework will alternatively use those two information and the coherence between them to find the global structure of the image.

2.3 Proposed Framework

The growth rings on otolith images correspond to ridges and valleys (together known as creases) in computer vision. Those are intuitively the relief curves of the landscape obtained when the image intensity is seen as a height map. As pointed out above, their perception is mainly the result of two grouping laws, one concerned about contrast, locating creases on local maxima or minima of intensity, the other being the good continuation, grouping together those loci forming curves long and smooth enough. In a first part of the algorithm the good continuation is exploited to compute a continuous orientation based family of curves, which in a second part is compared with contrast information to extract only the relevant creases. We should point out that both of those results are of interest for biological applications. While the computed family of curves correspond to the temporal history of the shapes of the otoliths, the extracted crease curves supply the actual growth rings. The different steps are outlined bellow, in relation with Figure 1, and will be detailed in the next section.

The first component of the proposed framework implements the good continuation principle for otoliths images. Good continuation is the grouping law that account for our viewing of continuous and smooth curves (Kanizsa, 1979). If perceptual cues have compatible directions, the curve to which they are all tangent will be seen as a unique curve. Orientation information has a key role and an interpolation based scheme is considered to estimate a dense orientation field. An example is shown Figure 1, top left. Details are in section 3.1. Then, given a prior model on accretionary growth, formalised as a dome-shaped potential function, the successive shapes of the otolith are reconstructed as being as tangent as possible to the orientation field. This model permits an embedding of time information in a third dimension satisfying both biological and psychovisual constraints. The result can be seen Figure 1, top right. The algorithm used will be detailed in section 3.2.

The implementation of the good continuation provides as an output a series of curves which are potential growth rings. A contrario detection is then exploited to combine this geometric information with a contrast based measure to detect crease curves. This step is illustrated figure 1, bottom right. Detail on a contrario detection and the measure used are found section 3.3. Intrinsically a contrario detection will detect several curves for a given growth rings, and an additional grouping law is required to fuse together the curves corresponding to a same structure. The result is seen Figure 1, bottom left. Section 3.4 will outline the algorithm used, full detail can be found in (Chessel, 2007).

As stressed previously, low level vision is about emergence by interaction. In the proposed implementation, those interactions comes from feedback loops, both positives and negatives. Section 3.5 describes how iteration can be used in place of those feedback loops to mimic the emergence process and allow for the progressive apparition of the structures we seek.

3 FROM GOOD CONTINUATION TO ITERATED MULTIMODAL A CONTRARIO DETECTION

3.1 Good Continuation via Orientation Interpolation

Good continuation has attracted much work in the computer vision community. Often an image of edgels -"edge elements", point supposed to be part of an curve along with the orientation of said curve

at that point- is taken as input, and continuous and smooth curves that link them are looked after (Parent and Zucker, 1989; Zweck and Williams, 2004).

Good continuation can be interpreted as an interpolation process. Either directly the interpolation of curves , Euler's elastica (Mumford, 1994) being then seen as a suitable and elegant solution, or through orientation interpolation. The idea is then to build, from a sparse edgel image, a dense orientation field where to each point is associated the tangent to an eventual structure going through that point. Curves in accordance with the good continuation principle are then the one the most tangent to that orientation field

In the case of otoliths, as outlined in the preceding section, such a field is particularly meaningful. The whole image can be described by concentric structures, and as such an orientation can be associated to each point. Furthermore, a biological interpretation can be associated: under the widely accepted hypothesis that variation of optical properties are linked to the biological growth, recovering the tangents to the structures means recovering the local direction of accretionary growth.

In (Chessel et al., 2006) two interpolation operators are presented. Orientation data belong to the unit circle $S^1 = \{x \in \mathcal{R}^2 \mid |x| = 1\}$. But extending data in S^1 poses additional challenges to extending scalar data. To the innate ambiguity of interpolation, one has to manage an ambiguity due to the periodic nature of S^1 and the need to use two maps to parametrize it. We then can distinguish two cases. Either the extension can be achieved by a laminar field, meaning one parametrisation is enough and the extension in S^1 is similar to the scalar case, or a turbulent field is needed and singularities are unavoidable. The hypothesis that can be made in the general case is that the field to be estimated is locally laminar: near each curvilinear structures a smooth field can be reconstructed, and far from them such an orientation field is meaningless. In the particular case of otoliths, a unique singularity is expected in the growth center.

The AMLE (Absolutely Minimizing Lipschitz Extension) is the extension operator used, it verifies an axiomatic approach (Chessel et al., 2006). It has been well studied mathematically. Existence and uniqueness has been proved in the scalar case ((Caselles et al., 1998) and its references). In particular, it verifies a maximality principle which guarantee that the solution is oscillation-free.

Let Ω be a subset of $\mathcal{R}^2$. Let S^1 be parametrise with the angle with the horizontal axis in $[0, pi[$. Let $D \subset \Omega$ be a set of points and/or curves and $\theta_0 : D \rightarrow S^1$. Then $\theta : \Omega \rightarrow S^1$ is the AMLE of θ_0 in Ω if:

$$\begin{cases} D^2\theta(D\theta, D\theta) = 0 \text{ in } \Omega, \\ \theta|_D = \theta_0 \text{ on } D, \end{cases} \quad (1)$$

i.e. if the second derivative in the direction of the gradient is equal to zero.

Numerically the equation was solved using the associated evolution problem. Because of the aforementioned ambiguity associated with the use of S^1, and the iterative nature of that scheme, a multi-resolution initialisation algorithm was used.

The set D of initial points can be obtained in various ways, as we will see later. An example of computed field can be seen Figure 1, the inital point being in black. The field is visualised via it's field lines using line integral convolition (Cabral and Leedom, 1993).

3.2 Recovering Shape Evolution

In this section is presented the representation of the otolith growth via its successive shapes and a way of computing such a representation from an image using the computed orientation field (Fablet et al., 2006). Such a representation stem from both biological modelling and computer vision constraint and algorithms. It is of interest both for itself, as the history of the shapes taken by the otolith, and as a mean of computing curves candidates to be growth rings, as used in the next section.

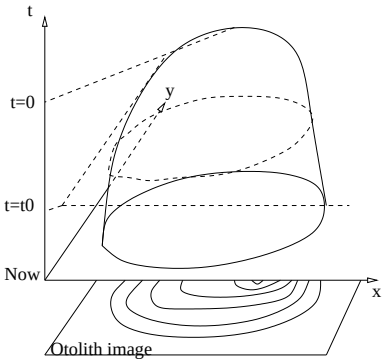

Figure 2: The successive shapes of the otoliths are represented as the level-lines of a dome shaped potential.

As suggested in the seminal work of D'arcy Thompson (D'arcy Thompson, 1917), we adopt a level-set setting to represent the accretionary growth process. It comes to introduce a potential function U defined over $\mathcal{R}^2$ such that the shape $\Gamma_t(U)$ of the considered biological structure within a given observation plane at time t is given by the level set of U,

$$\Gamma_t(U) = \{p \in \mathcal{R}^2 \text{ such that } U(p) = f(t)\}, \quad (2)$$

where f is a strictly monotonic continuous function (see Figure 2). Given U, the sequence of level sets $\{\Gamma_t(U)\}_{[0;T]}$ represents the evolution of the shape from time 0 to time T. This representation conforms to the classical assumption that accretionary growth is locally normal to the shape and thus that the shapes are included one in another (there is no reabsorbtion of the growth). But that representation also complies naturally to many of the low-level vision constraints defined earlier: thanks to it, we are bound to find smooth quasi-convex and concentric parallel curves.

The potential U is computed using a variational algorithm as the smooth potential following the previous definition that is the most tangent to θ, the orientation field computed section 3.1. Let I be the otolith image. Let θ be the computed orientation field with value in $[0,\pi[$. Then the hill-shaped potential function U, with minimum value 0 on the outline and maximum 1 in the center is computed as the minimum of an data driven regularized energy

$$U = \arg\min_U \int_{x\in\mathcal{R}^2} |\nabla U(x)|(1+\gamma\cdot\left\langle \frac{\nabla U(x)}{|\nabla U(x)|},\theta(x)\right\rangle^2)dx \quad (3)$$

It tends to align the tangents to the level-line of U to the computed field θ. The successive shapes of the otolith during its growth are then estimated via the successive and concentric level-sets of U.

3.3 A Contrario Detection

3.3.1 Principles

The a contrario detection relies on the Helmoltz principle, which states that a given geometrical structure in an image is perceptually meaningful if its probability of occurrence in a random image is low enough (Desolneux et al., 2003). Thus, given a collection of objects the assumption is made that they were randomly generated: a false random probability law is defined and meaningful objects are the ones that are unlikely enough with respect to this false model. It can be seen as an implementation of a perceptual grouping law, with the objects being the prospective perceptual groups and the random probability law defining the considered gestalt law.

Formally the a contrario detection is stated as follow. Let I be a grayscale image. Let $\mathcal{C}$ be a set of curves extracted from I and $\mathcal{C}_p$ the set of all pieces of curves from $\mathcal{C}$. Let M be a measure of creaseness (grayscale image) on I. Let $H(m) = \frac{1}{N}\#\{x|M(x) > m\}$, with $N = \#\{x \in I\}$, be the probability for a point of I to have a creaseness measure greater than m.

Definition 1 *Let $c \in \mathcal{C}_p$ be a curve of lenght l and $m = \min_{x\in c} M(x)$. The number of false alarms of that event is defined as*

$$NFA(c) = |\mathcal{C}_p| \times H(m)^l \quad (4)$$

Let $\varepsilon \in \mathcal{R}$. A given piece of curve c is said to be ε-meaningful if $NFA(c) < \varepsilon$.

Ultimately the detection is based on the length of the curves and the minimum of the creasness measure along them: between two curves with the same minimal contrast the more meaningful one will be the longer one.

The influence of ε has been shown to be small (Desolneux et al., 2003), such that a contrario detection can be considered to be parameterless.

The clear separation between the geometric structures being worked on and the random model telling us a contrario the relevant ones allows us to see the process as mutimodal (i.e. different cues brings in several distinct types of information). Indeed the geometric structures, which here are not generic but precomputed, are completely independent from the noise model, and are based on different geometric cues. Hence, if none the less a correlation between the two is detected, it stresses the existence of an underlying geometrical structure in the original image: what we are interested in is how much the two distinct informations ultimately describe the same object.

3.3.2 A Set of Candidate Curves

In the previous section was computed a continuous potential function U, implementing the good continuation principle. It will be used to give us a set of curves that are likely candidates for the growth rings we want to extract. Let $\Gamma_\lambda = \{x|U(x) = \lambda\}$ be the level-set of value λ of U, then if N is the wanted number of curves, we set

$$\mathcal{C} = \{\Gamma_\lambda|\lambda = \frac{k}{N}, k = 1...N\} \quad (5)$$

3.3.3 A Contrast based Measure

A lot of works have studied the local differential properties of images to define their ridges and valleys (Serrat et al., 2000; Sole et al., 2001). The two main criterion are maxima of intensity in the direction of the maximal curvature and maxima of level-line curvature.

Given the Hessian (the matrix of the second order derivatives), the chosen measure is the greatest hessian eigenvalue, or equivalently the greatest principal curvature. It is clear that it is maximal on the crease, it is not too localised contrary to the maxima of the level-line curvature and its sign allows us to differentiate ridges and valleys. The fact that it also responds

well on edges may be a drawback. But this is not problematic in our case as otoliths are rather flat images and the only edge in otolith image is the rim, which is treated separately anyway. So if λ_1 and λ_2 are the two eigenvalues of the hessian of I, associated with eigenvectors v_1 and v_2, $\lambda_1 > \lambda_2$, we define a ridge measure to be

$$M(x) = \lambda_1^+(x) = \begin{cases} \lambda_1(x) \text{ if } \lambda_1(x) > 0 \\ 0 \text{ else,} \end{cases} \quad (6)$$

and conversely λ_1^- for a valley measure.

3.4 Curve Fusion via Alpha Shapes

A contrario detection is about detection and not optimisation, thus a number of pieces of curves are detected as meaningful for a given crease. A step of grouping is necessary, which compute a unique curve from a given group. The detected curves are first regrouped into shapes, two curves being considered as in the same shape if their traces on the pixel grid are connex using 8-connexity. A regularized version of the shape is then computed by taking the α-*shape* of that boundary (Bernardini and Bajaj, 1997). That shape is then represented using triangulated polygon (Felzenszwalb, 2005) and the unique crease associated with a given group of detected curves is then defined as the medial axis of the triangulation. It will not be detailed further here, more details can be found in see (Chessel, 2007)),

3.5 Emergence via Iteration

It can be argued that both positive and negative feedback loops are a sine qua non condition of complex systems (Thomas and Thieffry, 1995). It is the fact that two or more perceptual cues can both reinforce and attenuate one another in non-linear and global ways that give rise to mid-level constructions, which in turn both give rise to global structures and get fed back to drive the individual cues interaction.

That process can be modelled using iterations, i.e. using the detected mid-level elements to drive the process of computing the global structure out of individual information. Contrarily to iterative schemes, used to solve partial differential equations for example, for which convergence and uniqueness results exist, complex systems are characterised by solutions that are difficult to predict analytically, but are rather simulated from given initial conditions.

Two perceptual information are used, orientation and contrast. The a contrario detection imposes to consider independent features, thus the feedback relies on orientation estimation only. The orientation interpolation step uses as input a set of points with known orientation. While initialisation is given by a simple filter, after an iteration of the proposed framework the extracted curves along with the tangent to these curves provides updated inputs to update the orientation field. Being the result of the combination of both perceptual informations, those tangents will allow us to compute orientation fields more closely following the structures, and thus to improve the results.

4 RESULTS

The presented algorithm were implemented in C/C++, using the Megawave2 (Froment, 1998) and the CGAL computational geometry library (CGAL Editorial Board, 2006) libraries. A simple filter selects interesting points to initialise the process. There are few parameters which are not crucial and can essentially be kept constant for a wide range of images.

Previous methods of 2D otoliths image analysis where limited to otolihs considered simple (like plaice, not shown here) and would fail on more complicated species like hake (Fig. 3 top). It is, as far as we known, the first time that reconstructing the history of the shapes as done here is attempted. Quantitative results with respect to synthetic data can found in (Chessel, 2007).

Results on otoliths from different fish species can be seen in Figures 3(a) and 3(b). For each are shown the dome shaped potential motolith, represented by its level lines, and the pieces of growth rings computed, both on top of the original image. Both are shown for the first iteration and after a few iterations.

The improvement over the iterations of the recovered shapes is clear. While at first cluttered by details not relevant with respect to the global structure sought after (on the left side of the hake otolith for exemple), a few iteration of comparing information from orientation and from contrast managed to disregard that local data and smooth the details out. On the growth rings however, that improvement is less visible. There may be two reasons. First those structure are less global than the whole shape evolution, and thus not as dependant over long range multimodal interaction. Second the probability law used in the a contrario detection is very conservative, being based on the minimum, and fail to recover long curves if they pass through a less contrasted part of the image.

5 CONCLUSIONS

Image analysis is one of the means of systematic analysis for the concentric structures found in otoliths. But automatic analysis is a challenge because of the noise and of the low contrast. Those structures are clear to human vision however, so a psychovisual analysis of low-level vision as a complex system was presented to understand how we manage to organise the atomistic information into a coherent whole.

It led us to an iterative algorithm which exploits the coherence between two distinct perceptual cues, orientation and contrast, to go back and forth between individual pixels and a global dome shaped potential. The results are good and biological applications that use them, including morphogenesis modelling and data fusion can be envisaged.

As far as computer vision is concerned, future work will in particular be focused a contrario laws that would allow for curve completion. Besides, the proposed level-sets representation of the otolith growth recover the geometry of the otolith, which provides a common framework for comparing and combining various otoliths features (opacity, growth, chemical signatures...) for the characterisation of individual life traits. To that end, statistical methods for comparing different features with respect to a given geometry will be needed.

To conclude, this work showed how specific computer vision development can be applied to a biological problem so that both computer vision and biology benefit from the cross-fertilisation such transdisciplinary studies induce.

REFERENCES

Benkirane, R., editor (2002). *La complexit, vertiges et promesses*. Le pommier.

Bernardini, F. and Bajaj, C. L. (1997). Sampling and reconstructing manifolds using alpha-shapes. In *Proc. 9th Canadian Conf. Computational Geometry*, pages 193–198.

Cabral, B. and Leedom, L. C. (1993). Imaging vector fields using line integral convolution. In *SIGGRAPH '93*, pages 263–270.

Caselles, V., Morel, J., and Sbert, C. (1998). An axiomatic approach to image interpolation. *IEEE Trans. Image Processing*, 7(3):376–386.

CGAL Editorial Board (2006). *CGAL-3.2 User and Reference Manual*.

Chessel, A. (2007). *Otolithe et Vision par Ordinateur*. PhD thesis, Universit de Rennes 1.

Chessel, A., Cao, F., and Fablet, R. (2006). Orientation interpolation: an axiomatic approach. In *European Conference on Conputer Vision*.

D'arcy Thompson, W. (1917). *On Growth and Form*. London press.

Desolneux, A., Moisan, L., and Morel, J.-M. (2003). A grouping principle and four applications. *PAMI*, 25(4):508–513.

Fablet, R., Pujolle, S., Chessel, A., Benzinou, A., and Cao, F. (2006). Variational level-set reconstruction of accretionary morphogenesis from images. In *IEEE International Conference on Image Processing*.

Felzenszwalb, P. F. (2005). Representation and detection of deformable shapes. *IEEE Transactions on Pattern Analysis and Machine Intelligence*, 27(2).

Froment, J. (1998). Megawave2. http://www.cmla.ens-cachan.fr/Cmla/Megawave/.

Guillau, A., Benzinou, A., Troadec, H., Rodin, V., and Le Bihan, J. (2002). Autonomous agents for edge detection and continuity perception on otolith images. *Image and Vision Computing*, 20(13):955–968.

Kanizsa, G. (1979). *Organization in Vision: Essays on Gestalt Perception*. Greenwood Publishing Group.

Mumford, D. (1994). Elastica and computer vision. In Bajaj, C., editor, *Algebraic Geometry and Its Applications*, pages 491–506. Springer-Verlag.

Panfili, J., de Pontual, H., Troadec, H., and Wright, P., editors (2002). *Manual of fish sclerochronology*. Ifremer-ird coedition.

Parent, P. and Zucker, W. (1989). Trace inference, curvature consistency, and curve detection. *IEEE Transactions on Pattern Analysis and Machine Intelligence*, 11(8):823–839.

Serrat, J., Lopez, A., and Lloret, D. (2000). On ridges and valleys. In *International Conference on Pattern Recognition ICPR'00*, pages 59–66.

Sole, A., Lopez, A., and Sapiro, G. (2001). Crease enhancement diffusion. *Comput. Vis. Image Underst.*, 84:241–248.

Thomas, R. and Thieffry, D. (1995). Les boucles de rtroaction, rouages des rseaux de rgulation biologiques. *Mdecine sciences*, 11(2):189–197.

Troadec, H., Benzinou, A., Rodin, V., and Le Bihan, J. (2000). Use of deformable template for two-dimensional growth ring detection of otoliths by digital image processing: - application to plaice (pleuronectes platessa) otoliths. *Fisheries Research*, 46(1):155–163.

Zweck, J. and Williams, L. (2004). Euclidian group invariant computation of stochastic completion fields using shiftable-twistable basis function. *J. Math. Imaging and Vision*, 21(2):135–154.

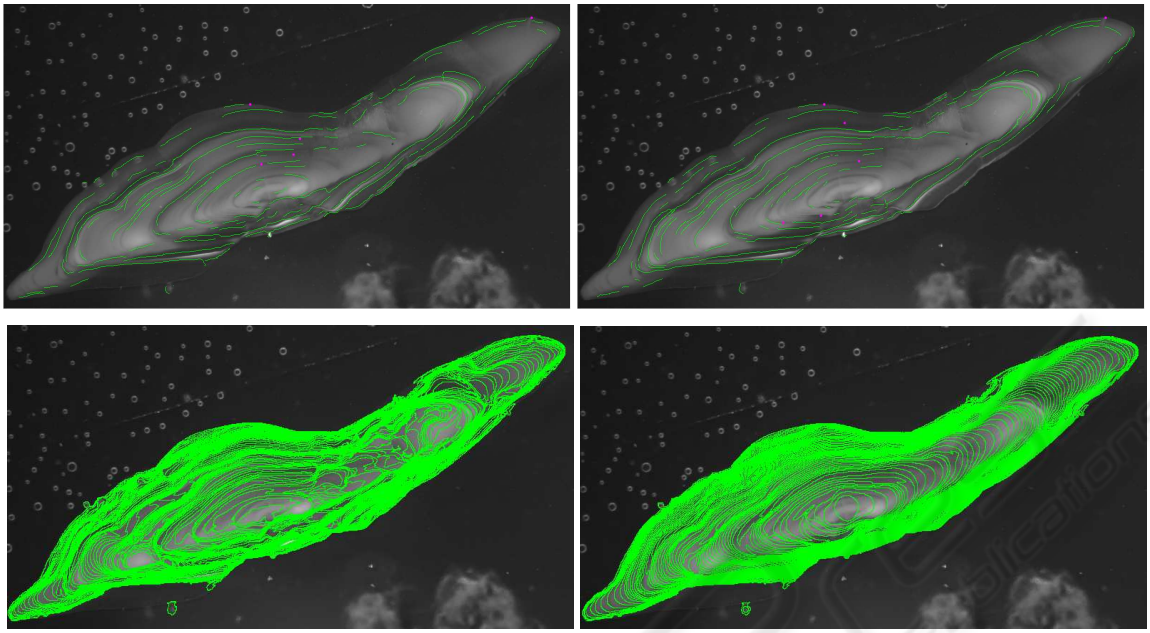

(a) A hake otolith, the recovered successive shapes (bottom), the extracted growth rings (top), first iteration (left), third iteration (right).

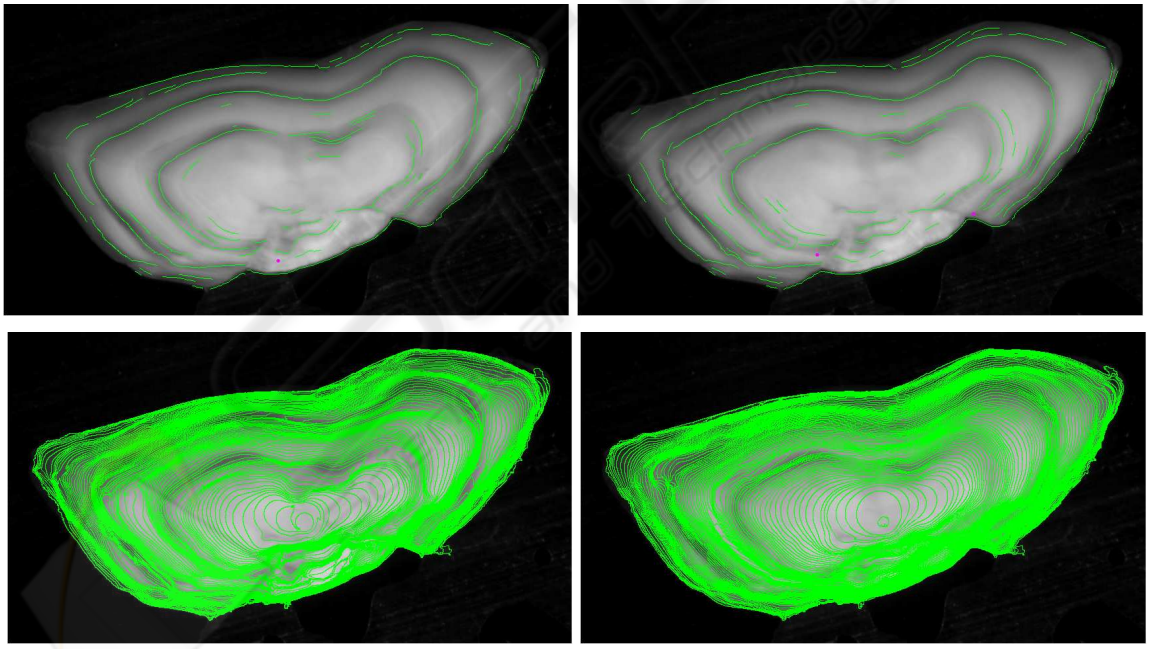

(b) A pollock otolith, the recovered successive shapes (bottom), the extracted growth rings (top), first iteration (left), third iteration (right).

Figure 3